Outcomes of the NIPPF Controller Linked to a Hybrid Rayleigh – Van der Pol-Duffing Oscillator

Y. A. Amer*, **A. T. EL-Sayed****, **M. N. Abd EL-Salam*****

*Department of Mathematics, Faculty of Science, Zagazig University, Zagazig, Egypt
**Department of Basic Sciences, Modern Academy for Engineering and Technology, Egypt
***Department of Basic Sciences, Higher Technological Institute, 10th of Ramadan City, Egypt
Corresponding author. E-mail: mansour.naserallah@yahoo.com (M. N. Abd EL-Salam)

Abstract: In this study, we presented a nonlinear integral positive position feedback controller (NIPPF) approach method that combines the advantages of both integral resonant controllers (IRC) and positive position feedback controllers (PPF) to control nonlinear systems. We adjusted the equation of a Hybrid Rayleigh – Van der Pol- Duffing oscillator by adding the nonlinear integral positive position feedback (NIPPF) to control the vibrating system. The system is presented by a three-degree-of-freedom (3-DOF) containing the cubic nonlinear term and an external force. For getting the solution from the first approximation, we applied the multiple scales method (MSM). Graphically and numerically, we studied the system before and after adding the NIPPF controllers at the worst resonance case 1:1 internal and primary ($\Omega \cong \omega_1, \omega_1 \cong \omega_2$). We used the MATLAB program to simulate the efficacy of different parameters on both the main system and NIPPF controllers.

Keywords: Van der Pol - Duffing oscillator; Nonlinear integral positive position feedback; Multiple scales method; Resonance case; Fixed point.

1. INTRODUCTION

The Duffing oscillator is used as a main type model for different engineering and physical problems such as electric circuit, oscillation of plasma, optical stability and the buckled beam (Guckenheimer et al., 1984; Siewe et al., 2006; Ueda, 1979, Trueba et al., 2003; Siewe et al., 2004; Lazzouni et al., 2006). Wen et al., 2016 presented two kinds of van der pol oscillator containing fractional order terms. The averaging method is used for obtaining the approximation solution. The additional stiffness coefficient is almost zero and the additional damping coefficient damping is almost the maximum value when the two kinds of van der pol fractional existed. Huang, 2018 used the nonlinear time delayed feedback controller to suppress the vibrations of van der pol oscillator. He studied the effectiveness of the feedback gain on bifurcation point numerically. Eissa and Amer, 2004 used a cubic displacement feedback control to control the vibrations of a cantilever beam to 33% from its uncontrolled value. The strategy of control is investigated in two different resonance cases primary and sub-harmonic cases.

The delayed feedback used to control bifurcation of a fractional predator-prey system by Huang et al., 2019. Barron, 2016 investigated the dynamically stable and unstable behaviour of the ring of coupled van der pol oscillators. He discussed numerically also, the amplitude of the oscillator increased if the stability conditions are not satisfied. Kimiaeifar et al., 2009 used the Homotopy analysis method to obtain the analytic solution for the first time on a single – well, double – well and double – hump van der pol – Duffing oscillator. Cveticanin et al., 2008 presented the Rayleigh equation with a cubic nonlinearity oscillator and they studied the following cases: positive linear and cubic coefficients, positive linear and negative cubic coefficients and negative linear and positive cubic coefficients. (Kumar et al., 2016; Kumar et al., 2017; Kumar et al., 2018), modified and studied the bifurcation of Van der Pol – Duffing – Rayleigh oscillator. Of great importance to restrained the vibrations of van der pol oscillator. The NIPPF controllers are considered as one of the important types of controllers, which used for controlling the vibrating systems. Refs. (Omidi and Mahmoodi, 2015; EL-Sayed and Bauomy, 2018), presented three kinds of control to suppress the vibrations of vibrating systems such that, the Integral resonant controllers (IRC), positive position feedback controllers (PPF) and the non-linear Integral Positive Position feedback (NIPPF). The eminent type of decreasing the vibrations is NIPPF type. PPF controller and multimode modified positive position feedback (MMPPF) controllers are used for deceasing the vibrations of a flexible beam and a collocated structure respectively (Jun, 2010; Omidi and Mahmoodi, 2015). Amer et al., 2018 used the non-linear saturation controller to suppress the vibrations of vertical conveyor on the simultaneous resonance case primary and internal 1:1. For the first and the second modes, the amplitude of controlled system is reduced about 240% and 600% from the amplitude of uncontrolled system. He et al., 2018 presented the flapping-wing robotic aircraft (FWRA) equations that are ODES and PDES with boundary conditions. The boundary control is used for suppressing the vibrations with out-put constraint of the (FWRA).

In this article, the vibrations of a hybrid Rayleigh – Van der Pol- Duffing oscillator exciting by external force are suppressed by using NIPPF controllers. A three-degree-of-freedom system is resolved by applying (MSM). The behaviour of the system without and with NIPPF controllers is simulated numerically. The influences of some chosen coefficients are illustrated numerically and analytically. The rapprochement between numeric and analytic solution is offered.

2. MATHEMATICAL MODELLING

Kumar et al., 2018, presented the equation of a hybrid Rayleigh – Van der Pol- Duffing oscillator as:

$$\ddot{u}-2\varepsilon\mu\omega_1\dot{u}(1-\beta u^2-\frac{\delta}{\omega_1^2}\dot{u}^2)+2\varepsilon\mu\omega_1^2ku^3+\omega_1^2u=0 \tag{1}$$

We adjusted the hybrid Rayleigh – Van der Pol- Duffing oscillator by adding an external force and NIPPF controller as shown in Fig.1 to minimize its vibrations as the following:

$$\ddot{u}+\omega_1^2u-2\varepsilon\mu\omega_1\dot{u}(1-\beta u^2-\frac{\delta}{\omega_1^2}\dot{u}^2)+2\varepsilon\mu\omega_1^2ku^3 = \varepsilon f\cos(\Omega t)+\varepsilon\lambda_1 v+\varepsilon\lambda_2 z \tag{2}$$

$$\ddot{v}+2\varepsilon\zeta\dot{v}+\omega_2^2 v=\varepsilon\gamma_1 u \tag{3}$$

$$\dot{z}+\sigma z=\gamma_2 u \tag{4}$$

where, the displacement of Van der Pol oscillator is u. The NIPPF controller's displacements are v and z. The coefficients of nonlinear terms are β, δ and k. ω_1, ω_2 are the natural frequencies of van der pol oscillator and NIPPF controller. The excitation amplitude and frequency are f, Ω. μ, ζ are the damping coefficients. The control signals are λ_1, λ_2. The gains are γ_1, γ_2. σ is the lossy integrator's frequency.

3. PERTURBATION TREATMENT

We applied the multiple scales method (Nayfeh and Mook, 2008) to obtain the solutions of equations (2)-(4):

$$u(t;\varepsilon)=u_0(T_0,T_1)+\varepsilon u_1(T_0,T_1) \tag{5}$$

$$v(t;\varepsilon)=v_0(T_0,T_1)+\varepsilon v_1(T_0,T_1) \tag{6}$$

$$z(t;\varepsilon)=z_0(T_0,T_1)+\varepsilon z_1(T_0,T_1) \tag{7}$$

The first and second derivatives take the forms:

$$\frac{d}{dt}=D_0+\varepsilon D_1+... \tag{8}$$

$$\frac{d^2}{dt^2}=D_0^2+2\varepsilon D_0D_1+... \tag{9}$$

For the first approximation solution, we performed a two time scales $T_r=\varepsilon^r t$ where, $D_r=\frac{\partial}{\partial T_r}$ (r = 0,1). Appending equations (5)-(9) into equations (2)-(4) and equating the coefficients of the same power of ε.

$O(\varepsilon^0)$:

$$(D_0^2+\omega_1^2)u_0=0 \tag{10}$$

$$(D_0^2+\omega_2^2)v_0=0 \tag{11}$$

$$(D_0+\sigma)z_0=\gamma_2 u_0 \tag{12}$$

$O(\varepsilon)$:

$$(D_0^2+\omega_1^2)u_1=-2D_0D_1u_0+2\mu\omega_1D_0u_0-2\mu\omega_1\beta(D_0u_0)u_0^2 -\frac{2\mu\delta}{\omega_1}(D_0u_0)^3-2\mu k\omega_1^2u_0^3+f\cos\Omega t +\lambda_1v_0+\lambda_2z_0 \tag{13}$$

$$(D_0^2+\omega_2^2)v_1=-2D_0D_1v_0-2\zeta D_0v_0+\gamma_1u_0 \tag{14}$$

$$(D_0+\sigma)z_1=-D_1z_0+\gamma_2u_1 \tag{15}$$

The formats of the solution of equations (10) and (11) are,

$$u_0=A_1(T_1)e^{(i\omega_1T_0)}+CC \tag{16}$$

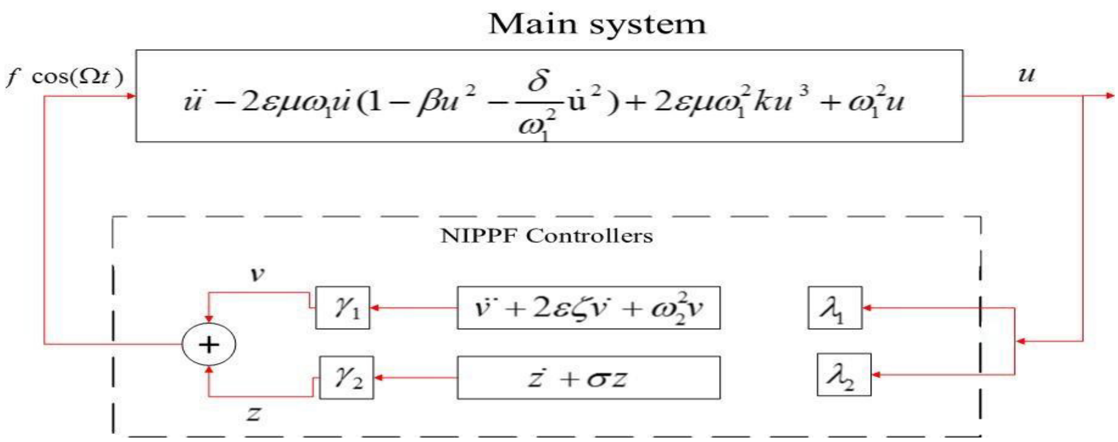

Fig.1. the flowchart diagram of the main system with NIPPF controllers.

$$v_0 = A_2(T_1)\,\mathrm{e}^{(i\,\omega_2 T_0)} + CC \tag{17}$$

To obtain the solution of equation (12), using equation (16) then,

$$z_0 = \gamma_2\left(\frac{\sigma - i\,\omega_1}{\sigma^2 + \omega_1^2}\right)A_1(T_1)\,\mathrm{e}^{(i\,\omega_1 T_0)} + H_1(T_1)\,\mathrm{e}^{(-\sigma T_0)} + CC \tag{18}$$

denote that A_n $(n = 1,2)$ and H_1, are complex functions in T_1. The complex conjugate parts collected in the term CC. For computation the right hand sides of equations (13) and (14), we will replace u_0, v_0 and z_0 by its values in equations (16)-(18) so that,

$$\begin{aligned}(D_0^2 + \omega_1^2)\,\mathrm{u}_1 = &\begin{pmatrix} -2i\,\omega_1 D_1 A_1 + 2i\,\mu\omega_1^2 A_1 \\ -2i\,\mu\omega_1^2(\beta + 3\delta)A_1^2\overline{A}_1 \\ -6\mu\omega_1^2 K A_1^2 \overline{A}_1 \\ +\dfrac{\lambda_2\gamma_2(\sigma - i\,\omega_1)}{(\sigma^2 + \omega_1^2)}\mathrm{A}_1 \end{pmatrix} e^{i\,\omega_1 T_0} \\ &-\left(2\mu\omega_1^2(k + i\,(\beta - \delta))\right)A_1^3 e^{3i\,\omega_1 T_0} \\ &+\left(\frac{f}{2}\right)e^{i\,\Omega T_0} + \left(\lambda_1 A_2\right)e^{i\,\omega_2 T_0} + CC\end{aligned} \tag{19}$$

$$\begin{aligned}(D_0^2 + \omega_2^2)\,\mathrm{v}_1 = &\left(-2i\,\omega_2 D_1 A_2 - 2i\,\zeta\omega_2 A_2\right)e^{i\,\omega_2 T_0} \\ &+\left(\gamma_1\,\mathrm{A}_1\right)e^{i\,\omega_1 T_0} + CC\end{aligned} \tag{20}$$

For getting the particular solutions of equations (19) and (20), we will remove the secular terms such that,

$$u_1 = M_1\,\mathrm{e}^{3\mathrm{i}\,\omega_1 T_0} + M_2\,\mathrm{e}^{\mathrm{i}\,\omega_2 T_0} + M_3 e^{i\,\Omega T_0} + CC \tag{21}$$

$$v_1 = M_4\,\mathrm{e}^{\mathrm{i}\,\omega_1 T_0} + CC \tag{22}$$

For the solution of equation (15), we will use equations (18) and (21) so that,

$$\begin{aligned}z_1 = &M_5\,\mathrm{e}^{\mathrm{i}\,\omega_1 T_0} + M_6\,\mathrm{e}^{3\mathrm{i}\,\omega_1 T_0} + M_7\,\mathrm{e}^{\mathrm{i}\,\omega_2 T_0} + M_8 e^{i\,\Omega T_0} \\ &+\left(K_1(T_1) - \sigma T_0 H_1(T_1)\right)e^{-\sigma T_0} + CC\end{aligned} \tag{23}$$

where M_∂ $(\partial = 1,\ldots,8)$ and K_1 offering complex functions in T_1 are mentioned in the appendix. From the first approximation, we concluded the following resonance cases:-

i) Primary resonance: $\Omega \cong \omega_1$
ii) Internal resonance: $\omega_1 \cong \omega_2$
iii) Simultaneous resonance: One-to-one internal and primary resonance.

4. PERIODIC SOLUTIONS

On this treatise, the selected one is simultaneous resonance $(\Omega \cong \omega_1, \omega_1 \cong \omega_2)$ is used to discuss the solvability conditions, we will introduce two detuning parameters (σ_1, σ_2) so that:

$$\Omega = \omega_1 + \varepsilon\sigma_1,\ \omega_2 = \omega_1 + \varepsilon\sigma_2 \tag{24}$$

Including equation (24) into equations (19) and (20) for compiling the solvability conditions as:

$$\begin{aligned}2i\,\omega_1 D_1 A_1 = &\,2i\,\mu\omega_1^2 A_1 - 2i\,\mu\omega_1^2(\beta + 3\delta)A_1^2\overline{A}_1 - 6\mu\omega_1^2 K A_1^2\overline{A}_1 \\ &+\frac{\lambda_2\gamma_2(\sigma - i\,\omega_1)}{(\sigma^2 + \omega_1^2)}A_1 + \frac{f}{2}e^{i\,\sigma_1 T_1} + \lambda_1 A_2 e^{i\,\sigma_2 T_1}\end{aligned} \tag{25}$$

$$2i\,\omega_2 D_1 A_2 = -2i\,\zeta\omega_2 A_2 + \gamma_1 A_1 e^{-i\,\sigma_2 T_1} \tag{26}$$

Exchanging all A_ℓ $(\ell = 1,2)$ by the polar form as:

$$A_\ell = \left({}^{a_\ell}\!/_2\right)e^{i\,\theta_\ell} \tag{27}$$

$$D_1 A_\ell = \frac{1}{2}(\dot{a}_\ell + \mathrm{i}a\,\dot{\theta}_\ell)e^{i\,\theta_\ell} \tag{28}$$

where θ_ℓ and a_ℓ $(\ell = 1,2)$ are the motion's steady state phases and amplitudes. Subjoining equations (27) and (28) into equations (25) and (26). For any two equal complex numbers, the real and the imaginary parts are equals so that:

$$\begin{aligned}\dot{a}_1 = &\left(\mu\omega_1 - \frac{\lambda_2\gamma_2}{2(\sigma^2 + \omega_1^2)}\right)a_1 - \left(\frac{1}{4}\mu\omega_1(\beta + 3\delta)\right)\mathrm{a}_1^3 \\ &+\left(\frac{f}{2\omega_1}\right)\sin\phi_1 + \left(\frac{\lambda_1}{2\omega_1}a_2\right)\sin\phi_2\end{aligned} \tag{29}$$

$$\begin{aligned}a_1\dot{\theta}_1 = &\left(-\frac{\lambda_2\gamma_2\sigma}{2\omega_1(\sigma^2 + \omega_1^2)}\right)a_1 + \left(\frac{3\mu k\,\omega_1}{4}\right)a_1^3 - \left(\frac{f}{2\omega_1}\right)\cos\phi_1 \\ &-\left(\frac{\lambda_1}{2\omega_1}a_2\right)\cos\phi_2\end{aligned} \tag{30}$$

$$\dot{a}_2 = (-\zeta)a_2 - \left(\frac{\gamma_1}{2\omega_2}a_1\right)\sin\phi_2 \tag{31}$$

$$a_2\dot{\theta}_2 = -\left(\frac{\gamma_1}{2\omega_2}a_1\right)\cos\phi_2 \tag{32}$$

where $\phi_1 = \sigma_1 T_1 - \theta_1, \phi_2 = \sigma_2 T_1 + \theta_2 - \theta_1$.

4.1 Fixed Point Solution

For steady-state solution, we maybe find the fixed point of the equations (29)-(32) by putting $\dot{a}_\ell = 0$ and $\dot{\phi}_\ell = 0$ so,

$$\begin{aligned}\left(\frac{\lambda_2\gamma_2}{2(\sigma^2 + \omega_1^2)} - \mu\omega_1\right)a_1 + \left(\frac{1}{4}\mu\omega_1(\beta + 3\delta)\right)\mathrm{a}_1^3 = &\left(\frac{f}{2\omega_1}\right)\sin\phi_1 \\ &+\left(\frac{\lambda_1}{2\omega_1}a_2\right)\sin\phi_2\end{aligned} \tag{33}$$

$$\sigma_1 a_1 + \left(\frac{\lambda_2\gamma_2\sigma}{2\omega_1(\sigma^2+\omega_1^2)}\right)a_1 - \left(\frac{3\mu k\,\omega_1}{4}\right)a_1^3 = -\left(\frac{f}{2\omega_1}\right)\cos\phi_1 - \left(\frac{\lambda_1}{2\omega_1}a_2\right)\cos\phi_2 \tag{34}$$

$$\left(-\zeta\right)a_2 = \left(\frac{\gamma_1}{2\omega_2}a_1\right)\sin\phi_2 \tag{35}$$

$$(\sigma_1-\sigma_2)a_2 = -\left(\frac{\gamma_1}{2\omega_2}a_1\right)\cos\phi_2 \tag{36}$$

Squaring then adding both sides of equations (35) and (36) to obtain the following equation:

$$\left(\zeta^2+(\sigma_1-\sigma_2)^2\right)a_2^2 = \left(\frac{\gamma_1 a_1}{2\omega_2}\right)^2 \tag{37}$$

By the same method with equations (33) and (34), one obtains the following:

$$\left\{\left(\frac{\lambda_2\gamma_2}{2(\sigma^2+\omega_1^2)} - \mu\omega_1\right)a_1 + \left(\frac{1}{4}\mu\omega_1(\beta+3\delta)\right)a_1^3 + \left(\frac{\lambda_1\omega_2\zeta a_2^2}{\omega_1\gamma_1 a_1}\right)\right\}^2 + \left\{\begin{matrix}\sigma_1 a_1 + \left(\frac{\lambda_2\gamma_2\sigma}{2\omega_1(\sigma^2+\omega_1^2)}\right)a_1 - \left(\frac{3\mu k\,\omega_1}{4}\right)a_1^3 \\ -\left(\frac{\lambda_1\omega_2(\sigma_1-\sigma_2)a_2^2}{\gamma_1\omega_1 a_1}\right)\end{matrix}\right\}^2 = \left(\frac{f}{2\omega_1}\right)^2 \tag{38}$$

4.2 Equilibrium Solution of a Fixed Point

While in movement to evolve the steady state solution's stability, start with the following procedures:

$$\left.\begin{matrix} a_m = a_{m0} + a_{m1}, \phi_m = \phi_{m0} + \phi_{m1} \\ \dot{a}_m = \dot{a}_{m1}, \dot{\phi}_m = \dot{\phi}_{m1}\end{matrix}\right\};(m=1,2) \tag{39}$$

Inserting equation (39) into equations (29)-(32) then, the following system is obtained:

$$\dot{a}_{11} = r_{11}a_{11} + r_{12}\phi_{11} + r_{13}a_{21} + r_{14}\phi_{21} \tag{40}$$

$$\dot{\phi}_{11} = r_{21}a_{11} - r_{22}\phi_{11} + r_{23}a_{21} - r_{24}\phi_{21} \tag{41}$$

$$\dot{a}_{21} = -r_{31}a_{11} + r_{32}\phi_{11} - r_{33}a_{21} - r_{34}\phi_{21} \tag{42}$$

$$\dot{\phi}_{21} = r_{41}a_{11} - r_{42}\phi_{11} + r_{43}a_{21} + r_{44}\phi_{21} \tag{43}$$

Rewrite the preceding system as:

$$\begin{bmatrix}\dot{a}_{11} & \dot{\phi}_{11} & \dot{a}_{21} & \dot{\phi}_{21}\end{bmatrix}^T = [J]\begin{bmatrix}a_{11} & \phi_{11} & a_{21} & \phi_{21}\end{bmatrix}^T \tag{44}$$

where the Jacobian J of the pervious system given by,

$$J = \begin{bmatrix} r_{11} & r_{12} & r_{13} & r_{14} \\ r_{21} & r_{22} & r_{23} & r_{24} \\ r_{31} & r_{32} & r_{33} & r_{34} \\ r_{41} & r_{42} & r_{43} & r_{44}\end{bmatrix} \tag{45}$$

where, $r_{\ell k}\,(\ell = 1,...,4 \text{ and } k = 1,...,4)$ are mentioned in the appendix. The eigen values of the Jacobian J are given by resolving the following determinant:

$$\begin{vmatrix} r_{11}-\lambda & r_{12} & r_{13} & r_{14} \\ r_{21} & r_{22}-\lambda & r_{23} & r_{24} \\ r_{31} & r_{32} & r_{33}-\lambda & r_{34} \\ r_{41} & r_{42} & r_{43} & r_{44}-\lambda \end{vmatrix} = 0 \tag{46}$$

which, are the roots of the following polynomial:

$$\lambda^4 + \Gamma_1\lambda^3 + \Gamma_2\lambda^2 + \Gamma_3\lambda + \Gamma_4 = 0 \tag{47}$$

where $\Gamma_i\,;(i=1,...,4)$ are the coefficients of equation (47) that, defined in the appendix. For the above system's solution to be stable, the Routh-Huriwitz criterion must be satisfied such that:

$$\Gamma_1 > 0, \Gamma_1\Gamma_2 - \Gamma_3 > 0, \Gamma_3(\Gamma_1\Gamma_2 - \Gamma_3) - \Gamma_1^2\Gamma_4 > 0, \Gamma_4 > 0 \tag{48}$$

5. NUMERICAL TREATMENT

We apply Runge-Kutta 4th order method using the MATLAB program for solving the main system's differential equation numerically after adding the NIPPF controllers. This study occurs in the worst resonance case (One-to-one internal and primary resonance). Fig. 2 (a), clarifies the amplitude of uncontrolled main system which, Approaching for three. For controlling the vibrations of main system, we used three types of controllers, PPF, IRC and NIPPF. The NIPPF controllers is the best type for controlling the vibrating system which, reduce the vibrations of the main system in a short time. It achieved success for diminishing the amplitude of the main system to reach 0.0002 that means the effectiveness of the NIPPF controller E_a =15000 (E_a =amplitude without controller/amplitude with controller) as shown in Fig.2 (d). In figure 3, the influence of the main system parameters (damping coefficient μ and nonlinearities coefficients β , δ and k) have been presented. From this figure, we note that, the amplitude of the main system is monotonic decreasing in the damping coefficient μ and nonlinearities coefficients β and k but monotonic increasing in the nonlinear coefficient δ . More increasing of the damping coefficient μ leads to saturation phenomena and the amplitude value equal to 0.9 so that, the system might need a control. The uncontrolled system investigated at three different values of the external force as shown in Fig. 4 from it, the main system will destroy by increasing the force amplitude therefore the main system must be controlled. Fig.6 represents the main system amplitude without and with

NIPPF controller, which is the suitable kind of controllers to suppress the vibrations of the main system.

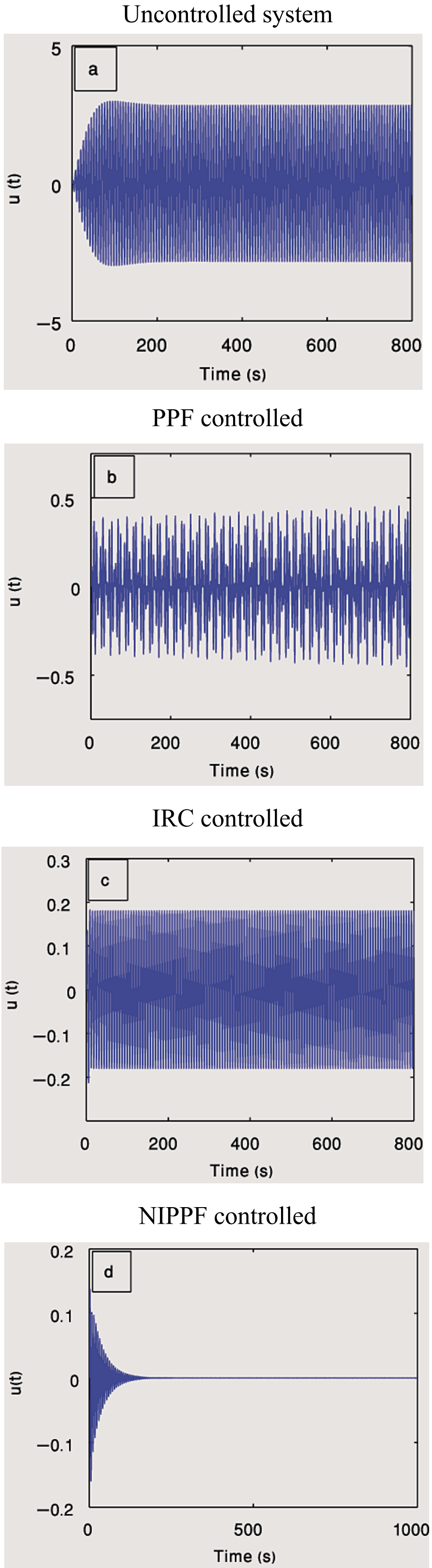

Fig. 2. Main system amplitude at the resonance case, (a) Uncontrolled system, (b) PPF Controlled, (c) IRC Controlled and (d) NIPPF Controlled.

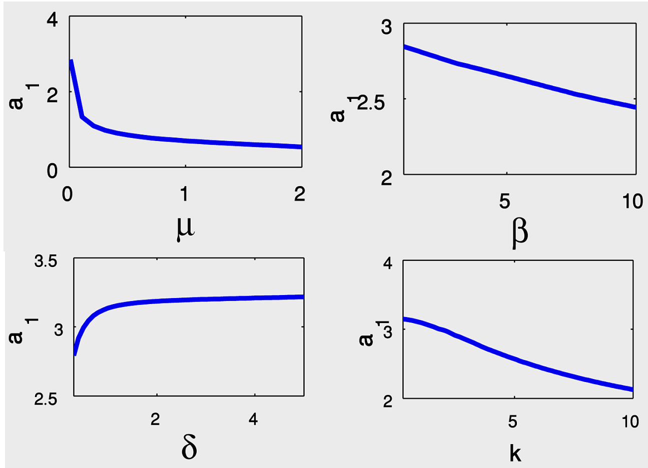

Fig. 3. The influence of the parameters of the main system without control.

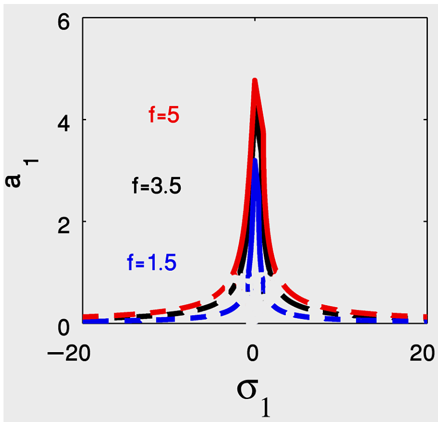

Fig. 4. The effect of the external force on the uncontrolled system.

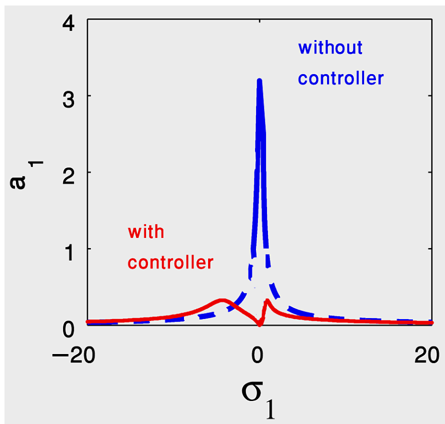

Fig. 5. The response curves of the main system without and with controller.

5.1 Frequency Response Curves of Controlled System

In this part, we illustrated the amplitudes of the main system and NIPPF controller against to the detuning parameter σ_1 for all parameters within the simultaneous resonance (one-to-one internal and primary resonance). The solid line refers to the stable solution while, the dash one refers to an unstable solution as shown in Fig.6. For increasing values of the external excitation force f , the amplitudes of the main system and NIPPF controller is also having increasing values as represented in Figs. 7a and 7b. For the small values of the natural frequency ω_1 , the bandwidth of the main system is wider. In addition, the amplitudes of the main system and NIPPF controller are monotonic decreasing on the natural frequency ω_1 as shown in Figs.8a and 8b. Confirmed on Figs 9a and 9b, the bandwidth of the main system amplitude is wider and NIPPF controller amplitude increasing for larger values of the feedback signal γ_1 . The amplitudes are decreased when the feedback signal γ_2 is increasing as illustrated in Figs. 10a and 10b. For large values of the control signal λ_1 , the bandwidth of the main system amplitude is wider as represented in Fig. 11a. The NIPPF controller's amplitude decreasing when the control signal λ_1 increasing as illustrated in Fig.11b. Fig. 12a illustrated that, the main system amplitude is increasing for the small values of control signal λ_2 . The NIPPF controller's amplitude is monotonic decreasing in the control signal λ_2 as shown on Fig. 12b. For increasing values of the lossy integrator's frequency σ , the amplitudes are also increasing as shown in figure 13.

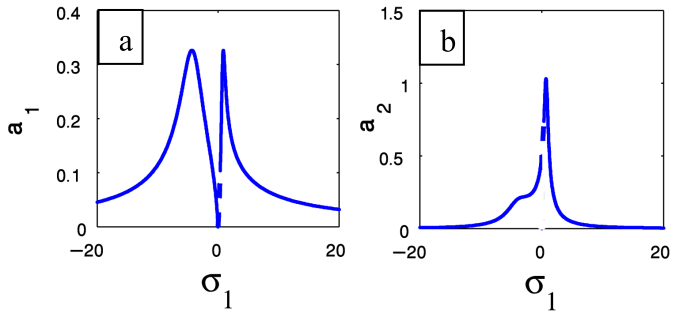

Fig. 6. Graphics of the response curves (a) the main system (b) the NIPPF controller.

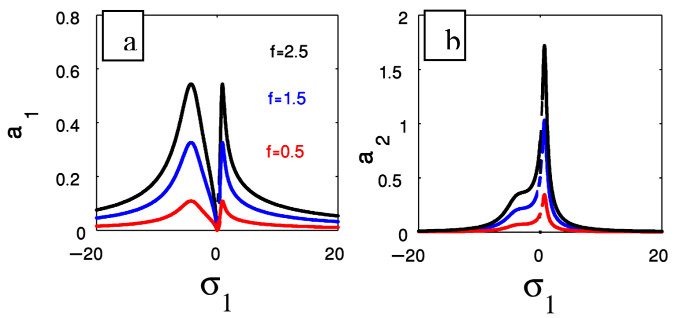

Fig. 7. External force efficacy on (a) the main system (b) the NIPPF controller.

From figure 14, the main system amplitude reaches to its minimum values when $\sigma_1 = \sigma_2$ as presented on Fig.14a and the amplitude of the NIPPF controller increasing and shift to right for increasing values of σ_2 according to Fig.14b.We confirm the numerical solutions of Eqs. (2)-(4) and the analytical solutions of Eqs. (29) - (32) as shown in figure 15. This rapprochement is orderly at the optioned resonance case when $\sigma_n = 0$ (n=1, 2) (i.e. $\Omega_1 \cong \omega_1$ and $\omega_1 \cong \omega_2$). The sold lines elucidated the numerical solution of Eqs. (2)-(4) while, dash lines elucidated the amplitude adjustments a_1 and a_2 for the generalized coordinates u and v . Finally, There is a good agreement between the numerical and analytical solutions of the main system from t=300 and for the NIPPF controller from t=100 and there is a good agreement between the numerical and analytical solutions for the response curves as presents in Fig.16.

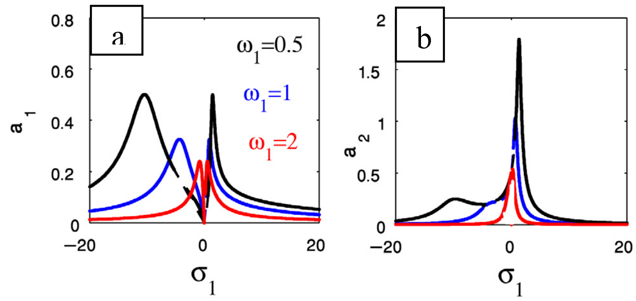

Fig. 8. Natural frequency efficacy on (a) the main system (b) the NIPPF controller.

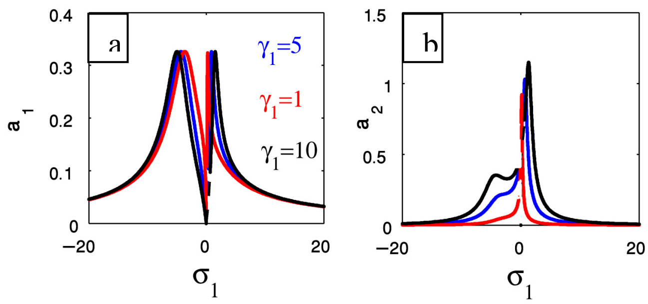

Fig. 9. Feedback signal γ_1 efficacy on (a) the main system (b) the NIPPF controller.

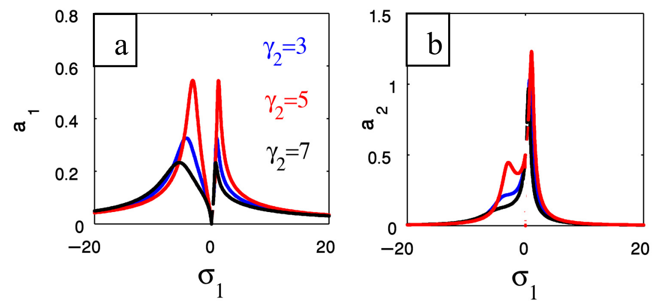

Fig. 10. Feedback signal γ_2 efficacy on (a) the main system (b) the NIPPF controller.

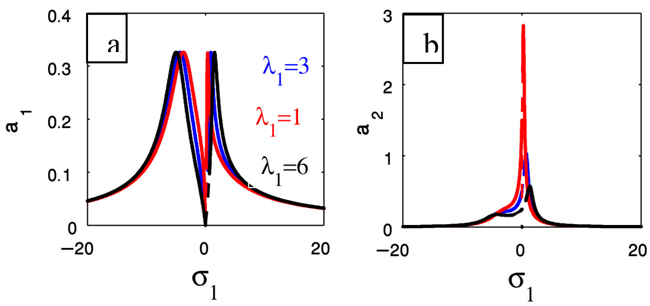

Fig. 11. Control signal λ_1 efficacy on (a) the main system (b) the NIPPF controller.

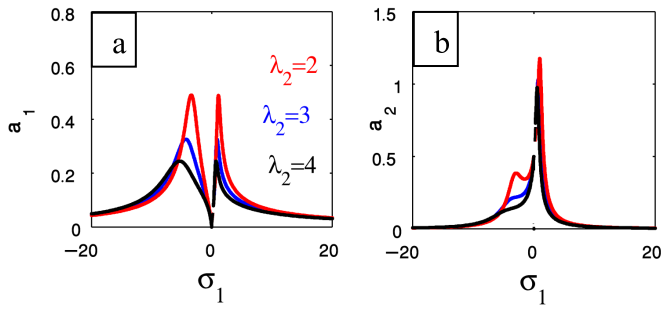

Fig. 12. Control signal λ_2 efficacy on (a) the main system (b) the NIPPF controller.

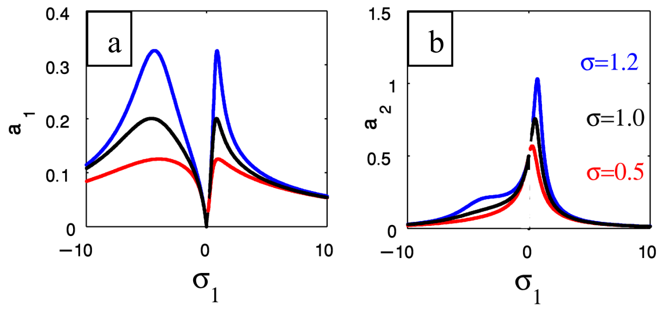

Fig. 13. Lossy integrator's frequency σ efficacy on (a) the main system (b) the NIPPF controller.

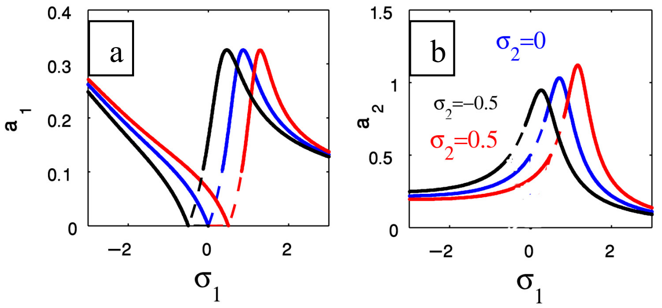

Fig. 14. Detuning parameter σ_2 efficacy on (a) the main system (b) the NIPPF controller.

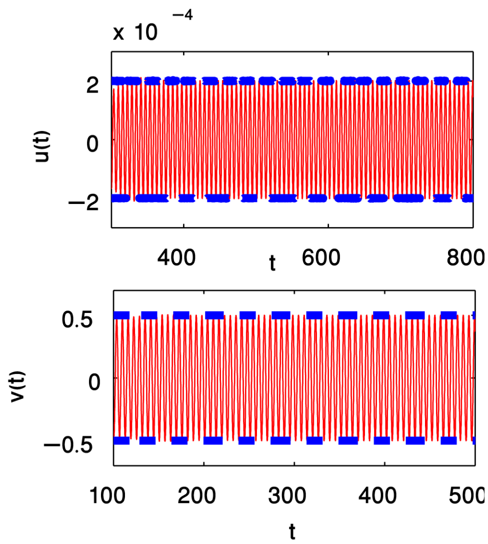

Fig. 15. Comparison between the numerical solution (———) and the perturbation analysis (--------) for the closed loop.

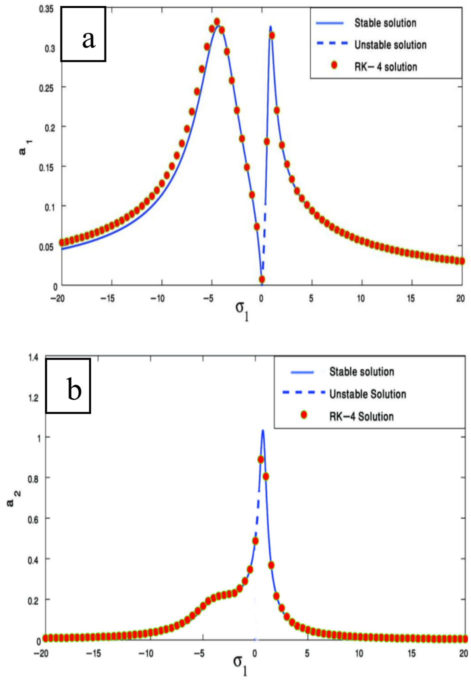

Fig. 16. Comparison between the FRC Solution and RK- 4 Solution.

6. CONCLUSION

Nonlinear integral positive position feedback (NIPPF) was introduced as a novel method that combines the advantages of both integral resonant controllers (IRC) and positive position feedback controllers (PPF) to control nonlinear systems. Moreover, one of its main advantages is to reduce vibrations in a short time as shown in Fig.2 (d) so, NIPPF controller was illustrated for the simultaneous resonance ($\Omega \cong \omega_1, \omega_1 \cong \omega_2$) of the Hybrid Rayleigh – Van der Pol-Duffing oscillator. The solution of the nonlinear system from the first approximation is obtained by applying the method of multiple scales. We succeed to reduce the vibrations of Van der Pol oscillator from three to 0.0002 by using NIPPF controllers that means the effectiveness of the NIPPF controller E_a =15000. The study divulged that:

1) Increasing the external force destroys the uncontrolled system and increasing the damping coefficient of the main system not enough to suppress the vibrations so, we used the NIPPF controllers.
2) Increasing the value of external excitation leads to increasing in the system and NIPPF amplitudes.
3) The amplitudes of the system and NIPPF are monotonic decreasing functions on the natural frequency ω_1, signal feedback γ_2 and control signal λ_2.
4) By increasing the value of the lossy integrator's frequency σ, the amplitudes of the main system and the NIPPF controllers are increasing.
5) The minimum amplitudes of the vibrating suspended cable occur when $\sigma_1 = \sigma_2$.

For the response curves, there is a good agreement between the FRC Solution and RK- 4 Solution.

REFERENCES

Amer, Y. A., EL-Sayed, A. T., & EL-Salam, M. A. (2018). Non-linear Saturation Controller to Reduce the Vibrations of Vertical Conveyor Subjected to External Excitation. *Asian Research Journal of Mathematics*, 1-26.

Barron, M. A. (2016). Stability of a ring of coupled van der Pol oscillators with non-uniform distribution of the coupling parameter. *Journal of applied research and technology*, 14(1), 62-66.

Cveticanin, L., El-Latif, G. A., El-Naggar, A. M., & Ismail, G. M. (2008). Periodic solution of the generalized Rayleigh equation. *Journal of Sound and Vibration*, 318(3), 580-591.

Eissa, M., & Amer, Y. A. (2004). Vibration control of a cantilever beam subject to both external and parametric excitation. *Applied mathematics and computation*, 152(3), 611-619.

El-Sayed, A. T., & Bauomy, H. S. (2018). Outcome of special vibration controller techniques linked to a cracked beam. *Applied Mathematical Modelling*, 63, 266-287.

Guckenheimer, J., & Holmes, P. (1984). Nonlinear oscillations, dynamical systems and bifurcations of vector fields. *J. Appl. Mech*, 51(4), 947.

He, W., Mu, X., Chen, Y., He, X., & Yu, Y. (2018). Modeling and vibration control of the flapping-wing robotic aircraft with output constraint. *Journal of Sound and Vibration*, 423, 472-483.

Huang, C. (2018). Multiple scales scheme for bifurcation in a delayed extended van der Pol oscillator. *Physica A: Statistical Mechanics and its Applications*, 490, 643-652.

Huang, C., Li, H., & Cao, J. (2019). A novel strategy of bifurcation control for a delayed fractional predator–prey model. *Applied Mathematics and Computation*, 347, 808-838.

Jun, L. (2010). Positive position feedback control for high-amplitude vibration of a flexible beam to a principal resonance excitation. *Shock and Vibration*, 17(2), 187-203.

Kimiaeifar, A., Saidi, A. R., Bagheri, G. H., Rahimpour, M., & Domairry, D. G. (2009). Analytical solution for Van der Pol–Duffing oscillators. *Chaos, Solitons & Fractals,* 42(5), 2660-2666.

Kumar, P., Narayanan, S., & Gupta, S. (2016). Investigations on the bifurcation of a noisy Duffing–van der Pol oscillator. *Probabilistic Engineering Mechanics*, 45, 70-86.

Kumar, P., Kumar, A., & Erlicher, S. (2017). A modified hybrid Van der Pol–Duffing–Rayleigh oscillator for modelling the lateral walking force on a rigid floor. *Physica D: Nonlinear Phenomena*, 358, 1-14.

Kumar, P., Kumar, A., Racic, V., & Erlicher, S. (2018). Modelling vertical human walking forces using self-sustained oscillator. *Mechanical Systems and Signal Processing*, 99, 345-363.

Lazzouni, S. A., Siewe, M. S., Kakmeni, F. M., & Bowong, S. (2006). Slow flow solutions and chaos control in an electromagnetic seismometer system. *Chaos, Solitons & Fractals*, 29(4), 988-1001.

Nayfeh, A. H., & Mook, D. T. (2008). Nonlinear oscillations. *John Wiley & Sons*.

Omidi, E., & Mahmoodi, S. N. (2015). Sensitivity analysis of the nonlinear integral positive position feedback and integral resonant controllers on vibration suppression of nonlinear oscillatory systems. *Communications in Nonlinear Science and Numerical Simulation*, 22(1-3), 149-166.

Omidi, E., & Nima Mahmoodi, S. (2015). Multimode modified positive position feedback to control a collocated structure. *Journal of Dynamic Systems, Measurement, and Control*, 137(5).

Siewe, M. S., Kakmeni, F. M., Bowong, S., & Tchawoua, C. (2006). Non-linear response of a self-sustained electromechanical seismographs to fifth resonance excitations and chaos control. *Chaos, Solitons & Fractals*, 29(2), 431-445.

Siewe, M. S., Kakmeni, F. M., & Tchawoua, C. (2004). Resonant oscillation and homoclinic bifurcation in a Φ^6-Van der Pol oscillator. *Chaos, Solitons & Fractals*, 21(4), 841-853.

Trueba, J. L., Baltanás, J. P., & Sanjuán, M. A. (2003). A generalized perturbed pendulum. *Chaos, Solitons & Fractals*, 15(5), 911-924.

Ueda, Y. (1979). Randomly transitional phenomena in the system governed by Duffing's equation. *Journal of Statistical Physics*, 20(2), 181-196.

Wen, S., Shen, Y., Li, X., & Yang, S. (2016). Dynamical analysis of Mathieu equation with two kinds of van der Pol fractional-order terms. *International Journal of Non-Linear Mechanics*, 84, 130-138.

APPENDICES

Coefficients of equations (21)-(23):

$$M_1 = \frac{\mu(k + i(\beta - \delta))}{4} A_1^3(T_1), M_2 = \frac{\lambda_1}{\omega_1^2 - \omega_2^2} A_2(T_1)$$

$$M_3 = \frac{f}{2(\omega_1^2 - \Omega^2)}, M_4 = \frac{\gamma_1}{\omega_2^2 - \omega_1^2} A_1(T_1),$$

$$M_5 = -i\gamma_2 \left(\frac{\sigma - i\omega_1}{\sigma^2 + \omega_1^2}\right)^2 A_1(T_1), M_6 = \gamma_2 \left(\frac{\sigma - 3i\omega_1}{\sigma^2 + 9\omega_1^2}\right) M_1$$

$$M_7 = \gamma_2 \left(\frac{\sigma - i\omega_2}{\sigma^2 + \omega_2^2}\right) M_2, M_8 = \gamma_2 \left(\frac{\sigma - i\Omega}{\sigma^2 + \Omega^2}\right) M_3$$

From the system of equations (33)-(36), the trigonometric functions can be written as:

$$\sin\phi_2 = \left(-\frac{2\omega_2\zeta a_2}{\gamma_1 a_1}\right), \cos\phi_2 = \left(-\frac{2\omega_2(\sigma_1 - \sigma_2)a_2}{\gamma_1 a_1}\right),$$

$$\sin\phi_1 = \left(\frac{2\omega_1}{f}\right)\left\{\begin{array}{l}\left(\frac{\lambda_2\gamma_2}{2(\sigma^2+\omega_1^2)} - \mu\omega_1\right)a_1 + \left(\frac{1}{4}\mu\omega_1(\beta+3\delta)\right)a_1^3 \\ +\left(\frac{\lambda_1\omega_2\zeta a_2^2}{\omega_1\gamma_1 a_1}\right)\end{array}\right\}$$

$$\cos\phi_1 = -\left(\frac{2\omega_1}{f}\right)\left\{\begin{array}{l}\sigma_1 a_1 + \left(\frac{\lambda_2\gamma_2\sigma}{2\omega_1(\sigma^2+\omega_1^2)}\right)a_1 - \left(\frac{3\mu k\,\omega_1}{4}\right)a_1^3 \\ -\left(\frac{\lambda_1\omega_2(\sigma_1-\sigma_2)a_2^2}{\gamma_1\omega_1 a_1}\right)\end{array}\right\}$$

The coefficients of equations (44)-(47), take the following forms:

$$r_{11} = \left(\mu\omega_1 - \frac{\lambda_2\gamma_2}{2(\sigma^2+\omega_1^2)} - \frac{3}{4}\mu\omega_1(\beta+3\delta)\,a_{10}^2\right),$$

$$r_{12} = \left(\frac{f}{2\omega_1}\cos(\phi_{10})\right), r_{13} = \left(\frac{\lambda_1}{2\omega_1}\sin(\phi_{20})\right), r_{14} = \left(\frac{\lambda_1}{2\omega_1}a_{20}\cos(\phi_{20})\right),$$

$$r_{21} = \left(\frac{\sigma_1}{a_{10}} + \frac{\lambda_2\gamma_2\sigma}{2\omega_1(\sigma^2+\omega_1^2)a_{10}} - \frac{9\mu k\,\omega_1}{4}a_{10}\right),$$

$$r_{22} = -\left(\frac{f}{2\omega_1 a_{10}}\sin(\phi_{10})\right), r_{23} = \left(\frac{\lambda_1}{2\omega_1 a_{10}}\cos(\phi_{20})\right).$$

$$r_{24} = -\left(\frac{\lambda_1 a_{20}}{2\omega_1 a_{10}}\sin(\phi_{20})\right), r_{31} = -\left(\frac{\gamma_1}{2\omega_2}\sin(\phi_{20})\right),$$

$$r_{32} = 0, r_{33} = -(\zeta), r_{34} = -\left(\frac{\gamma_1 a_{10}}{2\omega_2}\cos(\phi_{20})\right),$$

$$r_{41} = \left(\frac{\sigma_1}{a_{10}} + \frac{\lambda_2\gamma_2\sigma}{2\omega_1(\sigma^2+\omega_1^2)a_{10}} - \frac{9\mu k\,\omega_1}{4}a_{10} - \frac{\gamma_1}{2\omega_2 a_{20}}\cos(\phi_{20})\right),$$

$$r_{42} = -\left(\frac{f}{2\omega_1 a_{10}}\sin(\phi_{10})\right), r_{43} = \left(\frac{\sigma_2-\sigma_1}{a_{20}} + \frac{\lambda_1}{2\omega_1 a_{10}}\cos(\phi_{20})\right),$$

$$r_{44} = \left(\left(\frac{\lambda_1 a_{10}}{2\omega_2 a_{20}} - \frac{\lambda_1 a_{20}}{2\omega_1 a_{10}}\right)\sin(\phi_{20})\right).$$

The polynomial's coefficients in equation (51), take the following forms:

$$\Gamma_1 = -(r_{11}+r_{22}+r_{33}+r_{44})$$

$$\Gamma_2 = r_{11}r_{22}+r_{11}r_{33}+r_{11}r_{44}+r_{22}r_{33}-r_{13}r_{31}-r_{12}r_{21} + r_{22}r_{44}+r_{33}r_{44}-r_{34}r_{43}-r_{24}r_{42}-r_{14}r_{41}$$

$$\Gamma_3 = r_{14}r_{41}(r_{22}+r_{33})+r_{24}r_{42}(r_{11}+r_{33})+r_{34}r_{43}(r_{11}+r_{22}) + r_{44}(r_{13}r_{31}+r_{12}r_{21}-r_{22}r_{33}-r_{11}r_{33}-r_{11}r_{22})$$

$$\begin{aligned}\Gamma_4 = {} & r_{11}(r_{23}r_{34}r_{42}-r_{24}r_{33}r_{42}-r_{22}r_{34}r_{43}+r_{22}r_{33}r_{44}) \\ & + r_{12}(r_{24}r_{33}r_{41}-r_{24}r_{31}r_{43}+r_{21}r_{34}r_{43}-r_{23}r_{34}r_{41}+r_{23}r_{31}r_{44}-r_{21}r_{33}r_{44}) \\ & + r_{23}(r_{22}r_{34}r_{41}-r_{21}r_{34}r_{42}+r_{24}r_{31}r_{42}-r_{22}r_{31}r_{44}) \\ & + r_{14}(r_{21}r_{33}r_{42}+r_{22}r_{31}r_{43}-r_{22}r_{33}r_{41}-r_{23}r_{31}r_{42})\end{aligned}$$